Forest Ecology and Management 357 (2015) 206–219

Contents lists available at ScienceDirect

Forest Ecology and Management

journal homepage: www.elsevier.com/locate/foreco

Ecosystem carbon (CO_2 and CH_4) fluxes of a *Populus dettoides* plantation in subtropical China during and post clear-cutting

Shenghua Gao [a], Jiquan Chen [b], Yuxi Tang [c], Jing Xie [d], Rui Zhang [e], Jie Tang [c], Xudong Zhang [a,*]

[a] State Key Laboratory of Tree Genetics and Breeding, Research Institute of Forestry, Chinese Academy of Forestry, Beijing 100091, China
[b] Center for Global Change and Earth Observations (CGCEO) and Department of Geography, Michigan State University, East Lansing, MI 48823, USA
[c] Hunan Academy of Forestry, Changsha 410004, China
[d] Beijing Forestry University, Beijing 100083, China
[e] State Key Laboratory of Urban and Regional Ecology, Research Center for Eco-Environmental Science, Chinese Academy of Sciences, Beijing 100085, China

ARTICLE INFO

Article history:
Received 1 April 2015
Received in revised form 16 August 2015
Accepted 19 August 2015

Keywords:
GHG flux
Carbon balance
Eddy covariance
Poplar plantation
Harvest effect
Forest regeneration

ABSTRACT

Poplar plantations have widely spread around the world due to its high productivity and adaptability. Clear-cutting is the primary harvesting method for poplar plantation management in southern China. However, the effect of harvesting on ecosystem carbon fluxes limits our ability to estimate its carbon sequestration. A consecutive, three-year observation on ecosystem CO_2 and CH_4 flux (F_{CO2} and F_{CH4}) of a *Populus dettoides* plantation on the floodplain of Yangtze River was made prior and post to the clear-cutting using an eddy-covariance system. We found that clear-cutting turned the ecosystem from a strong carbon sink to a mediate carbon source only in several months, July to next January, after the harvest. The ecosystem turned to a net carbon sink at the beginning of the first growing season following clear-cutting due to the large productivity of understory vegetation in this region. The annual carbon budget was -424.3 ± 52.5 g-C m^{-2} (95% confidence interval) in the harvesting year, with -53.6 ± 22.8 g-C m^{-2} the first year and -290.7 ± 34.2 g-C m^{-2} the second year after clear-cutting. Clear-cutting turned the ecosystem from a net CH_4 sink to a net CH_4 source after the third month, but during the three years the CH_4 emission only balanced out a very small portion (0.3%) of F_{CO2}. In non-inundation periods, F_{CH4} varied from -0.01 to 0.24 mmol m^{-2} d^{-1}, with a mean (±SD) of 0.11 ± 0.08 mmol m^{-2} d^{-1}, while it ranged from 0.33 to 4.39 mmol m^{-2} d^{-1} during inundation, with a mean (±SD) of 2.17 ± 1.16 mmol m^{-2} d^{-1}. Daily and weekly F_{CH4} during non-inundation period were highly correlated with ground water table, soil moisture, and friction velocity, while F_{CH4} during inundation depended on inundation depth.

1. Introduction

Poplar is well known for its large wood production, ability to adapt to different environments, and integration and synergy with agriculture (Coaloa and Nervo, 2011; Sannigrahi et al., 2010; SFA, 2013). Traditionally, poplar plantations have always been established for timber production (Coaloa and Nervo, 2011; Vietto et al., 2011; Xiao et al., 2013). Logically, it would be ideal for carbon sequestration purposes (Cannell and Milne, 1995; Xiao et al., 2013) and as a bioenergy supplier for mitigating climate change (Kauter et al., 2003; Sannigrahi et al., 2010; Sevigne et al., 2011; Wright, 2006). Xiao et al. (2013) analyzed the carbon sequestration capabilities of different ecosystems in China and reported that poplar plantations in subtropical China have a higher capability than other forest ecosystems in other regions of China. Even in the same climate zone, the carbon sequestration of a 7-year-old poplar plantation (-874 g-C m^{-2} yr^{-1}) (Xiao et al., 2013) in the subtropical region of China was also higher than that of a 13-year-old fir plantation (-255 g-C m^{-2} yr^{-1}) (Zhao et al., 2011), a 20-year-old coniferous plantation (~600 g-C m^{-2} yr^{-1}) (Liu et al., 2005), and a *Phyllostachys pubescens* forest (-668 g-C m^{-2} yr^{-1}) (Sun et al., 2013a). Yet, the capacity of production or potential as a bioenergy supplier in poplar plantations, in regards to their ability in climate change mitigation, needs to be further examined at longer temporal scales.

Harvest, an important activity in forest management, always has significant effects on carbon balance (Chen et al., 2004, 2014). After harvesting, sites are initially sources of CO_2, but eventually become sinks for CO_2 in the years following reforestation (Amiro et al., 2010; Fredeen et al., 2007). Over time, the carbon

* Corresponding author at: Research Institute of Forestry, Chinese Academy of Forestry, 1st Dongxiaofu, Haidian District, Beijing, China.
E-mail address: Zhxdcaf@163.com (X. Zhang).

http://dx.doi.org/10.1016/j.foreco.2015.08.026
0378-1127/

emission induced by harvest and other management activities would balance out part of the carbon uptake during forest growing, especially in production and bioenergy plantations which always have a shorter rotation. Nave et al. (2010) reported that harvesting reduced soil carbon by an average of 8 ± 3% (95% CI), according to the result of meta-analysis of 432 temperate forest harvest studies around the world. Clear-cutting is a traditional harvest practice that is widely applied in forest management throughout the world (Keenan and Kimmins, 1993; Ma et al., 2013; Rosenvald and Lohmus, 2008). Numerous studies have reported that clear-cutting turned the ecosystem from carbon sinks to carbon sources (Fredeen et al., 2007; Machimura et al., 2005; Takagi et al., 2009). The carbon emission after clear-cutting ranged from 200 to 1300 g-C m^{-2} yr^{-1} (Clark et al., 2004; Kowalski et al., 2004; Takagi et al., 2009), and the emission state lasted for either 3–10 years (Clark et al., 2004; Fredeen et al., 2007) or even 20 years (Law et al., 2001).

Clear-cutting does not only lead to CO_2 emission, but also affects F_{CH4} (Huttunen et al., 2003; Lavoie et al., 2013; Lindroth et al., 2012; Sun et al., 2011; Sundqvist et al., 2014). A majority of studies reported that clear-cutting turned the soil from net CH_4 sinks to net CH_4 sources (Lindroth et al., 2012; Sun et al., 2011; Sundqvist et al., 2014). However, Lavoie et al. (2013) found that clear-cutting increased CH_4 uptake at two Atlantic temperate forests in Nova Scotia, Canada. The different effects of clear-cutting on carbon balance in previous studies may be due to the differences of vegetation composition and/or climate. Clear-cutting is an important harvest method in the temperate and subtropical forests of China (Ma et al., 2013). Presently, the studies of clear-cutting's effect on carbon balance in subtropical regions of China are mainly focused on soil-atmospheric balance (Guo et al., 2010; Ma et al., 2013; Tang et al., 2006; Yang et al., 2005), with few conducted at ecosystem scale. The harvest effect on production and bioenergy plantations requires more attention as harvesting is frequently performed in short rotation plantations, which would cause a large carbon emission and draw down the capacity of carbon sequestration in these plantations at a broader temporal scales.

The Yangtze River is the longest river in China and the third longest river in the world, with a floodplain of more than 5000 km^2 in the middle and lower reaches. Since the 1980s, poplar plantations have been widely promoted on the floodplain in the middle and lower reaches of Yangtze River. It serves not only as a timber production plantation but also as a protection against snails and schistosomiasis (Sun et al., 2009; Zhang et al., 2006). *Populus dettoides* is the most common tree species in this region. Generally, the rotation time of a poplar plantation is around 10 years with the required tending during the first two years. The immature poplar plantations at this site have a large CO_2 uptake (Xiao et al., 2013) and the soil of a mature stand shows an obvious absorption of CH_4 in non-inundated growing season (Gao et al., 2013). However, because of a high ground water table (Chen, 1996; Johnson and McCormick, 1979) and seasonal inundation, it may be a hotspot of methane (Dinsmore et al., 2009; Hagedorn and Bellamy, 2011), resulting in a high uncertainty in estimating carbon balance on the floodplains.

Based on the three-year consecutive observation taken before/after the harvesting on a floodplain in the middle reaches of Yangtze River, we aim to answer the following questions: (1) Will clear-cutting turn the field into a net carbon source? If so, when will the new plantation become a net carbon sink? (2) What is the magnitude and character of the ecosystem F_{CH4} on the floodplain of this region and how important is the CH_4 budget in the whole carbon balance within a riparian poplar plantation? (3) What are the significant biophysical drivers responsible for the changes?

2. Materials and methods

2.1. Site description

Our study site is located on the floodplain in the middle reaches of the Yangtze River (29°31′35″N, 112°55′22″E, 31 m asl, Fig. 1), with a subtropical monsoon climate and prevailing wind from north (Fig. 1). The long-term, mean annual temperature was 16.8 °C and the mean annual precipitation was 1400 mm. The soil was fluvo-aquic soil, with 13.6 and 9.9 g kg^{-1} organic carbon in the upper 40 and 100 cm, respectively. Generally, the field was inundated for 20–50 days a year, with the longest record of 130 days.

The mature plantation was afforested with different poplar clones of *P. dettoides* in 2000 in an area of 60 ha, with spacing of 4 × 5 m. It was clear-cut without stump removal during May–August 2011 due to frequent rain in spring and summer. In late July, the trees within 500 m of the tower were all felled. The canopy height of mature plantation was ~19.5 m, and the average diameter at breast height was 0.23 m, with dominant understory species of *Leonurus arternisia* with a coverage of ~90%. Nearly all the trunks, branches and ~50% of foliage of the trees were removed from the site, with an overall removal biomass of 69.83 t ha^{-1}. The residual belowground and aboveground biomass was 13.11 and 5.40 t ha^{-1}, respectively (Appendix A). From July 2011 to January 2012, the clear-cut was predominantly covered by *Cynodon dactylon*, *Viola verecunda*, *Polygonum flaccidum*, and *Clinopodium gracile*. The site was afforested in late January–early February 2012 with 1-year-old *P. dettoides* seedings at the same density. Herbicide was implemented from May through June, 2012. The average canopy height in the beginning of 2012, 2013 and 2014 was 3.5, 4.5 and 7.0 m, respectively. The field was inundated from July 11th to August 20th, 2012, but not inundated in the year of 2011 or 2013. During the periods of September 2012–March 2013, and April–November 2013, the field was intercropped with Chinese-cabbage (*Brassica pekinensis*) and pumpkin (*Cucurbita moschata*), respectively, in order to increase the economic returns.

2.2. Instruments and measure methods

The eddy-covariance (EC) method was used to measure F_{CO2} and F_{CH4}. The EC system includes a sonic anemometer (CSAT3; Campbell Scientific, Logan, UT, USA) to measure the three-dimensional wind components and sonic virtual temperature, an open-path CO_2/H_2O infrared gas analyzer (LI-7500; LI-COR Biosciences, Lincoln, NE, USA) to measure CO_2/H_2O concentrations and pressure, and a close-path fast methane analyzer (DLT-100; Los Gatos Research, Mountain View, CA) to measure CH_4 concentration. The CSAT3, LI-7500, and the inlet of DLT-100 were separated by ~20 cm from each other. The measurement height was adjusted according to the canopy height. Generally, the observation height was 2–3 m higher than the canopies in the beginning of each growing season, resulting in 21, 3.5, 6.5, and 7.5 m in January–June in 2011, July 2011–February 2012, March 2012–February 2013, and March 2013–February 2014, respectively. Observation height was adjusted to 3.5 m on July 4th, 2011, when the trees in the south of the tower and the trees within 50 m of the tower in other directions were all felled. The LI-7500 was calibrated in laboratory every 6 months.

Methane flux was observed since late September 2011 when the mature trees in the research area had all been felled. DLT-100 was based on the off-axis ICOS (off-axis Integrated Cavity Out-put Spectroscopy) technique, which can enlarge the laser beam path to kilometers in the measuring cell by the highly-reflective mirrors, so that the ultra-weak absorption can be captured (Hendriks et al., 2008). The sampled air was drawn to the

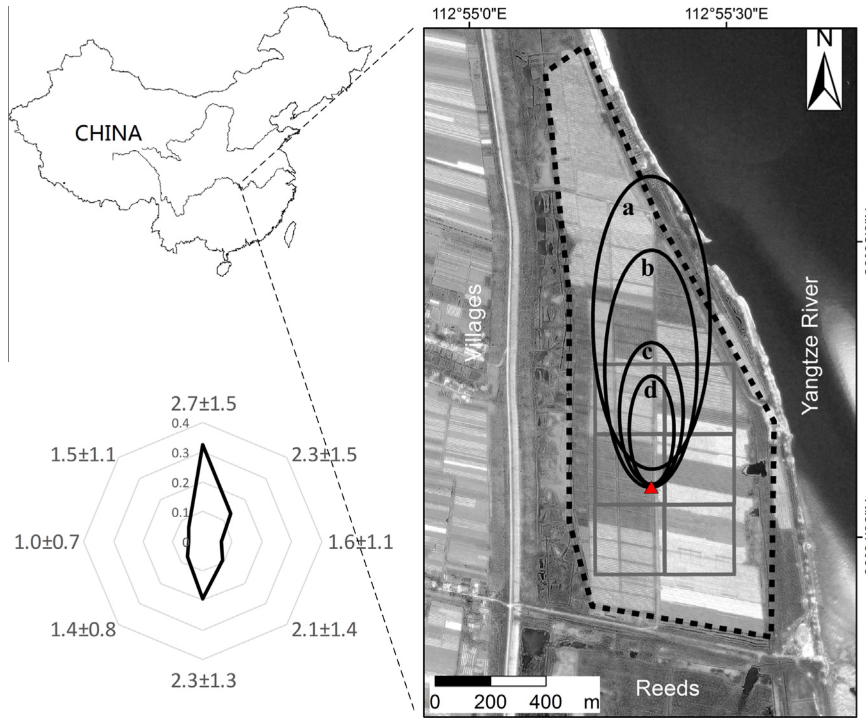

Fig. 1. Map and wind-rose diagram of the study site. The black dot-dot polygon is the region of interest, and the red triangle was the location of the tower. The six gray squares indicate the 250 × 250 m^2 pixels of NDVI (MYD13Q1) from MODIS. The solid ellipses marked with a, b, c, and d represent the footprints of before clear-cutting (January–June 2011, daytime), after clear-cutting (August 2011–February 2012, 24 h), the first (March 2012–February 2013, 24 h) and the second year (March 2013–February 2014, 24 h) of the young plantation, respectively. The footprints are calculated with the model of Schmid (1994). (For interpretation of the references to color in this figure legend, the reader is referred to the web version of this article.)

DLT-100 measuring cell by a scroll vacuum pump (XDS-35i, Edward, MA, USA) through a 7.5-m long metal tube (inner diameter ~9 mm, with Teflon material covering the inside wall). A 5 μm and a 1 μm membrane filter was applied, respectively, at the inlet and outlet of the tube in order to keep the mirrors clear enough for a longer time, though there was a 2 μm steel filter inside the DLT-100. The mirror ring-down time (MRT) was kept no less than ~7 μs and the cell pressure was set to ~190 hPa (Hendriks et al., 2008). The mirrors were cleaned every 1–2 months when the DLT-100 was calibrated with ~2.0 $\mu L\ L^{-1}$ standard gas. The sealing accessories of XDS35i were changed in order to maintain the pump in a good condition in February 2013.

A suite of environmental variables were also directly measured. The photosynthetically active radiation (PAR, mmol m^{-2}) was observed with a quantum sensor (LI-190SB; Campbell Scientific, Inc., USA), while the sun plus sky radiation (R_g, W m^{-2}) was measured with a silicon pyranometer (LI-200X; Campbell Scientific, Inc., USA). A net radiometer (CNR-1; Kipp and Zonen, Delft, Netherlands) was used to record net radiation (R_n, W m^{-2}). A temperature and relative humidity probe (HMP45C; Campbell Scientific, Inc., USA) was used to measure air temperature (T_a, °C) and humidity (RH, %) at the height of LI-7500, and a tipping bucket rain gauge (TE525; Campbell Scientific, Inc., USA) was applied to measure precipitation (P, mm). Soil temperatures (T_s, °C) were measured by three temperature probes (107-L, Campbell Scientific, Inc., USA) at 5, 10, and 20-cm depth, and soil volumetric water contents (VWC, %) were measured by two water content reflectometers (CS616-L, Campbell Scientific, Inc., USA) at a 15-cm depth. Three soil heat flux plates (HFT3, Campbell Scientific, Inc., USA) at 2-cm depth were used to determine surface soil heat flux (G, W m^{-2}). The ground water table (WT, m) was observed by water level data logger (HOBO; Onset Computer Corporation, USA). Lastly, the Yangtze River water level (YRWL) at this site was averaged from two long-term observation stations (Jianli Station and Chenglingji Station, ~30 km upstream and ~50 km downstream from this site, respectively).

2.3. Flux calculation and QA/QC

Fluxes were calculated with the EdiRe software (Version 1.5.0.32; R. Clement, University of Edinburgh, UK; http://www.geos.ed.ac.uk/abs/research/micromet/EdiRe/), and a 30-min interval was chosen as the average. The values beyond 4-time standard deviation were removed as spikes. The double rotation (DR) was applied to correct the coordinate tilt (Rebmann et al., 2012). The time lags between the scalars (both LI-7500 and DLT-100) and the vertical wind component were estimated by a cross-correlation analysis method. However, the lag time between the CH_4 concentration and vertical wind component appeared ambiguous with this procedure. Consequently a constant lag time was used when no reasonable lag time was obtained. The constant lag time was first estimated from the tube length, the inner diameter, and the pump flow (Rebmann et al., 2012) and, then validated by the distribution of obtained lag time. Schotanus-correction was performed to converse buoyancy flux to sensible heat flux (Schotanus et al., 1983). The *Frequency Response* procedure of the EdiRe was used for correcting the loss due to frequency by sensors path, sensors separation and tube attenuation (Massman, 2004). The WPL correction (Webb et al., 1980) was applied to CO_2, CH_4, and latent heat flux, but temperature correction term was not applied for F_{CH4} because the temperature fluctuations were assumed to be attenuated by the tube (Ibrom et al., 2007).

Several additional steps were taken for F_{CH4} quality assurance. The DLT-100 timestamp differentiation was applied to detect the repeated records, which occurred frequently when the sample rate was <10 Hz and DLT-100 or the external pump was not working. The records were also deleted when the cell pressure was not in a reasonable range (184–197 hPa), such as when the DLT-100 calculation flag was not zero, the MRT was <6.5 μs, or CH_4 concentration was not in a reasonable range (1.7–3.5 ppm). When the record-keeping ratio was <92% after the aforementioned steps, this average interval would be omitted.

Additional steps were carried out for quality control of the half-hourly fluxes. First, the record in nighttime was removed when friction velocity (U_{star}) was less than 0.14, 0.10, 0.10, and 0.12 m s^{-1} in the periods of January–June in 2011, July 2011–February 2012, March 2012–February 2013, and March 2013–February 2014. We estimated these thresholds following Schmid (2003). Briefly, we first partitioned the nighttime F_{CO2} into different classes according to U_{star} values that was graded at 0.1 intervals, and then determined the proper threshold when F_{CO2} was stable. Footprints, integral turbulence characteristics, and stationarity tests of the covariance of vertical velocity and CO_2 concentration were calculated for every averaging interval by the internal subroutine of the EdiRe software. Footprint was used to estimate the contribution ratio of interesting area, and the fetch in each direction was specified. When contribution ratio was <70% before clear-cutting and <80% after clear-cutting, F_{CO2} and F_{CH4} of that 30-min interval would be removed, because F_{CO2} from the mature plantation is significantly larger than that from other fields around it. Additionally, if integral turbulence characteristics or stationarity test was >100%, F_{CO2} of this interval was deleted. In the end, the overall data coverage was 43.9% and 30.5% for F_{CO2} and F_{CH4}, respectively.

During May–August 2011, the fetch length was specified each day according to the progress of felling. When the contribution ratio was <80%, the 30-min fluxes were deleted. As a consequence, the fluxes from the un-felled field were kept only in May–June, while the fluxes from the cutover were kept only in July and August.

2.4. Gap-filling and uncertainty assessment

The small gaps (<2.5 h) of F_{CO2} were filled by the linear interpolation method, while the large gaps were filled by the nonlinear regressions (NLR) method (Falge et al., 2001). The entire research period was divided into small intervals with a 1–2 month window, according to the state of the field (e.g. clear-cutting and inundation). Gaps in daytime and nighttime were filled separately. First, the Lloyd & Taylor function (Falge et al., 2001; Lloyd and Taylor, 1994) was used to simulate the nighttime F_{CO2} which was supposed to be a nighttime ecosystem respiration (ER). The obtained parameters were used to fill the nighttime gaps and calculate the daytime ER, assuming consistency of temperature sensitivity between the nighttime and daytime exchanges (Xie et al., 2014). Then the Michaelis–Menten function was used to simulate daytime F_{CO2}, and the obtained parameters were used to fill the daytime gaps of F_{CO2} (Falge et al., 2001). Gross ecosystem production (GEP) was calculated as ER minus F_{CO2}.

There does not exist a widely-acceptable method for F_{CH4} gap-filling. Zona et al. (2013) used a linear extrapolation to determine the cumulative F_{CH4} and a multiple imputation (MI) technique (Hui et al., 2004) to estimate the confidence intervals, while Chu et al. (2014) adopted the marginal distribution sampling method. Both methods are based on the Monte Carlo technique. In this study, we first applied the linear interpolation method to fill the small gaps (<2.5 h), and then used a Gliding-Window Mean Diurnal Variations (MDV) method to fill the large gaps (Falge et al., 2001). Our reason for using the MDV to fill the gaps of F_{CH4} is that the mean diurnal variation of F_{CH4} exhibited some similar pattern in some months and years, and the gaps did not always randomly distribute in a day (Gao et al., 2015). The window size was set to 7, 15, and 30 days, successively. Gaps larger than 30 days (because of instruments malfunction) were not filled. After gap-filling, daily flux was calculated from the daily averaged flux multiplied by 24 h. Monthly net exchange was calculated from the average daily F_{CH4} multiplied by the number of days for the month, and the gap of monthly-scale data was filled with a linear interpolation method. Additionally, cumulative fluxes were also calculated from the half-hourly dataset that was not gap-filled in the same way. These were used to examine the difference between the two methods. The annual budget was accumulated from monthly means.

The uncertainty of cumulative F_{CH4} and F_{CO2} was estimated by the multiple imputation (MI) method (Hui et al., 2004). MI is one of the Monte Carlo techniques in which the missing values are replaced by several simulated values and the uncertainty can be derived from the gap-filled datasets (Zona et al., 2013). MI has been used in EC data to fill the gaps in F_{CO2}, latent heat, sensible heat fluxes (Hui et al., 2004), as well as F_{CH4} and F_{N2O} (Zona et al., 2013). In this study, MI was implemented with the "Amelia-II" R-package (Honaker et al., 2011; Zona et al., 2013). In order to prove the simulations, "date" was set as the time series variable and "time" was set as the cross-sectional variable. The 95% confidential interval (95% CI) was calculated following Hui et al. (2004). However, only the uncertainty in the gap-filling was estimated.

2.5. F_{CH4} using static chamber prior to the harvesting

Prior to DLT-100 installation at the EC tower, measurements of F_{CH4} at the cutover and uncut field were carried out with six $0.6 \times 0.6 \times 1.6$ m static transparent chambers (three chambers at each site) from April through July, 2011 during clear-cutting to examine the short-term effects of clear-cutting on F_{CH4} (Gao et al., 2013). During August–September (i.e., after the clear-cutting), F_{CH4} was measured only in the clearcut. The understory plants were enclosed in the chambers. The observations were carried out every two hours for 24 h typically on sunny days each month in order to estimate the monthly fluxes. The daily F_{CH4} obtained from the chamber measurements was used to estimate the ecosystem F_{CH4} in 2011, though the F_{CH4} measured by chamber method was not exactly the ecosystem F_{CH4} because tree effect on F_{CH4} remains unclear. In January–June, the F_{CH4} from uncut field were used, while in July–September the F_{CH4} from the cutover were used in estimating the yearly F_{CH4}. The monthly fluxes from January to March were estimated from April through June by using a linear extrapolation method.

2.6. Normalized difference vegetation index (NDVI)

The 16-day NDVI data (MYD13Q1) of the Moderate Resolution Imaging Spectroradiometer (MODIS) with a spatial resolution of 250 m were adopted to quantify the vegetation dynamic. The NDVI data were obtained from the Land Process Distributed Active Archive Center, US Geological Survey, USA (http://www.usgs.gov/) (Chu et al., 2014). The NDVI within the research area was averaged from the values of six 250×250 m^2 centered on the tower (Fig. 1). The middle date of each 16-day period was used to represent this period. The data were converted to daily data by linear interpolation.

2.7. Statistical analysis

The potential environmental controls on half-hourly/daily/weekly F_{CH4} were initially explored with the Spearman correlation coefficient before modeling the F_{CH4} at different scales with stepwise linear regression method. In the end, half-hourly T_s, VWC, WT, GEP, U_{star}, R_n, G, and VPD were chose as the initial variables for modeling F_{CH4} at half-hourly to weekly scale with >50 data points for each week, while average T_s, VWC, WT, GEP, U_{star}, VPD, and NDVI were used for modeling F_{CH4} at daily to seasonal/

yearly scales. Non-linear regression was applied to examine the relationship between F_{CH4} and WT by filled/unfilled half-hourly F_{CH4} in June–September of 2012 and 2013. Two-sample *T*-test for the Means was used to identify the significance of the difference between fluxes in different periods. Unless specified, the significant level was set to 0.05 and uncertainty (±) always referred to a 95% CI. The 95% CIs of monthly/annual fluxes were obtained from MI by the method of (Hui et al., 2004), except annual F_{CH4} of 2011 that was propagated from the uncertainties of every month. For estimating GHG flux that is equivalent to F_{CO2}, F_{CH4} ($F_{CH4\text{-}CO2eq}$) was 28 times that of F_{CO2} according to the global warming potential of CO_2 and CH_4 in a 100-year horizon (Hartmann et al., 2013). We did not account for N_2O emission that may induced by crop cultivation. Statistical analyses were carried out by SAS 9.3 (SAS Institute Inc., Cary, NC, USA).

3. Results

3.1. Microclimate

The year 2012 had the lowest annual mean T_a of the past 30 years according to the long-term records at Wuhan meteorological station, ~145 km away for the research site. The annual average/maximum T_a of 2012 was 15.9/35.4 °C, which was lower than that in 2011 (16.8/37.1 °C) and 2013 (17.7/36.7 °C) (Fig. 2a). Yet, average/maximum T_s was 20.0/31.3, 17.3/32.0, and 15.2/32.0 °C in the three years, respectively. The field experienced the wettest year in 2012 of the three years, with 91% of the precipitation in the year concentrated in the first eight months. Regardless, the VWC remained at a higher level in the latter half of 2012 than that in 2011 and 2013 due to the occasional irrigations, frequent drizzle, and coverage of cabbage. During inundation, T_s was ~25 °C while VWC remained at the saturation of ~60% during July 11th–August 20th, 2011 (Fig. 2). WT appeared to be controlled by YRWL (Fig. 2e), which varied significantly throughout the seasons. The maximum WT in the three years was −2.49 (July 10th, 2011), +2.8 (July 31st, 2012), and −0.57 m (June 7th, 2013), respectively. WT rose significantly from −4.7 to −2.5 m after clear-cutting within four days (Fig. 2e). However, it cannot be attributed to clear-cutting only because YRWL were changing during this time as well. Interestingly, both in 2013 and 2014, there was a decrease in T_a in early February after a long time climbing up in January (Fig. 2a).

3.2. Vegetation change

NDVI was clearly influenced by the clear-cutting and cultivation actives (Fig. 3a). Overall, NDVI reached the smallest (0.2–0.3) of a year in winter, except in 2013 when cabbage was cultivated and NDVI remained at ~0.45. However, clear-cutting, young forest trending (e.g., weeding), soil preparation, and crop harvest always led to a decrease of NDVI, which recovered quickly in 1–2 weeks

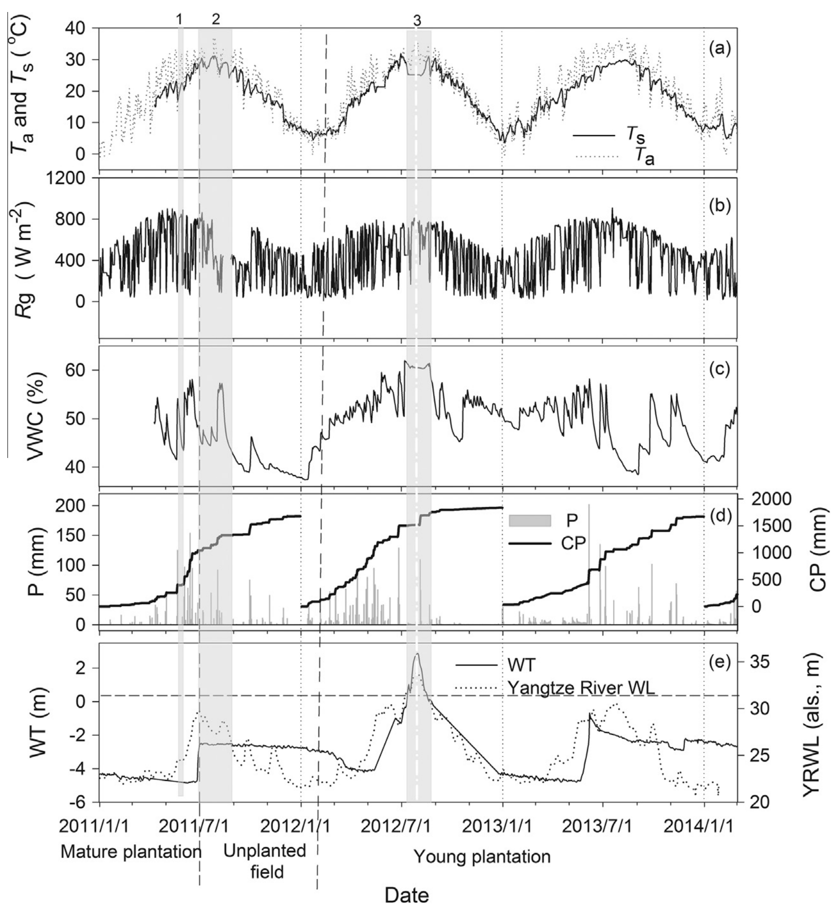

Fig. 2. The daily micrometeorological variables at the research site, including (a) the maximal air and soil temperature (T_a and T_s), (b) maximum solar radiation (R_g), (c) mean soil volumetric water content (VWC), (d) daily and accumulative precipitation (*P* and CP), and (e) ground water table (WT) and the Yangtze River's water level (YRWL). The 1st and 2nd shaded bars indicate the period of clear-cutting activities implemented in both late May and from July to August 2011, respectively. The 3rd shaded bar indicates the inundation period (11th July–20th August 2012). The left gray dash line indicates the beginning of observation in the clear-felled field, while the right gray dash line indicates the beginning of the young plantation. The dotted lines are the border of the years. The white dash-dotted line indicates the time of the highest WT.

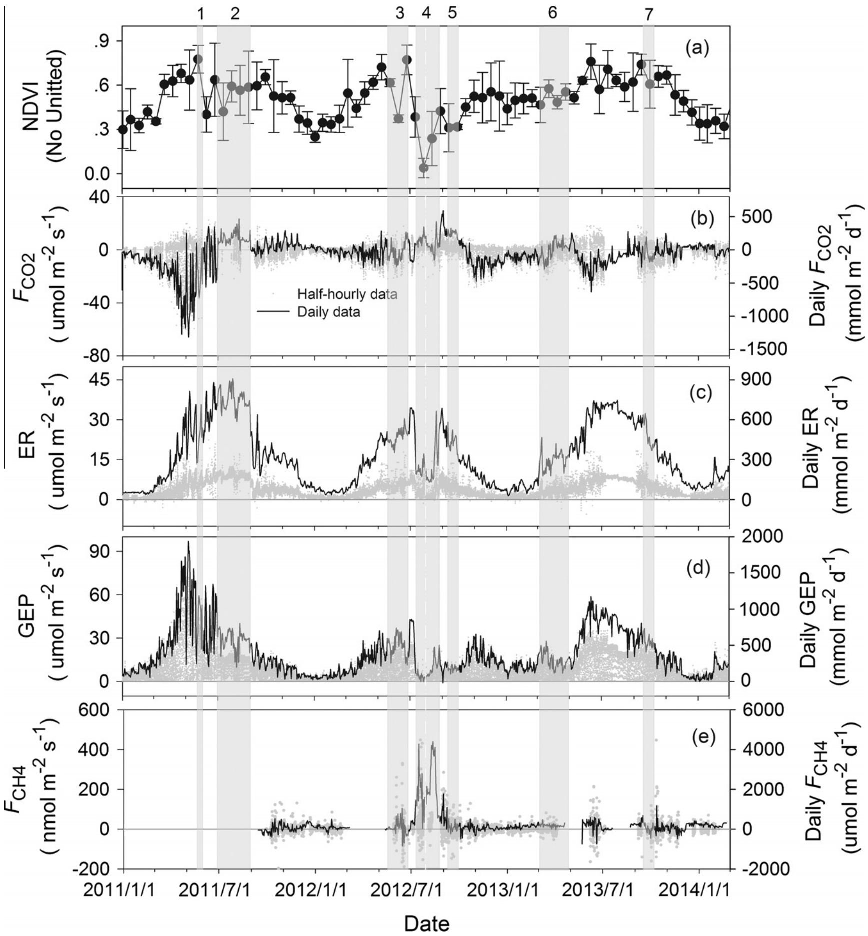

Fig. 3. Changes in: (a) 16-day NDVI (MYD13Q1), (b) half-hourly and daily CO_2 fluxes (F_{CO2} and Daily F_{CO2}), (c) half-hourly and daily ecosystem respiration (ER and Daily ER), (d) half-hourly and daily gross ecosystem production (GEP and Daily GEP), and (e) the half-hourly and daily F_{CH4}. NDVI (mean ± SD) was averaged from the six 250×250 m^2 gray squares indicated in Fig. 1. The 1st and 2nd shaded gray bars indicate the period of clear-cutting activities implemented in late May and from July to August 2011, respectively. The 3rd shade bar indicates the period of weeding with herbicide for young plantation tending. The 4th bar indicates the inundation period, while the white dash-dotted line indicates the time of highest WT. The 5th bar indicates the periods of the first month of cabbage cultivation. The 6th bar indicates the months of cabbage harvest and the beginning of pumpkin cultivation. The 7th bar indicates the month of pumpkin harvest.

due to the fast growth of understory vegetation. Inundation caused the NDVI to decrease dramatically when all of the herbage and even some of the poplar canopy were submerged when WT was higher than 2.0 m. During intercropping (September 2012–November 2013), NDVI fluctuated around 0.45–0.65, including the winter. Overall, the largest NDVI of the young plantation was only slightly smaller than that of the mature plantation (Fig. 3a); and the variation of understory vegetation in 2013 had insignificant effects on NDVI than in 2012 because the poplar canopy was better developed in 2013. It is important to mention that the dramatic decrease in NDVI in late May 2011 was mainly caused by a burst of *Clostera anachoreta* rather than clear-cutting, since only a very small patch of trees were felled in May. In addition, the obvious decrease in June 2012 was due to the weeding in May through June 2012.

3.3. Dynamics of CO_2 flux

Clear-cutting had significant effects on F_{CO2} (Fig. 3b–d). The maximum GEP of the cutover in July and August decreased to ~40% (803 mmol m^{-2} d^{-1} on August 12th) of that prior to the clear-cutting (1881 mmol m^{-2} d^{-1}), while ER did not decrease. As a result, the cutover turned to a net source of CO_2 in these two months. Three months after the clear-cutting, ER and GEP both decreased because of the approaching non-growing season. Thus, F_{CO2} fluctuated around zero and the cutover was a net weak CO_2 source until the arrival of next growing season when it became a net weak sink.

The young forest growth and intercropping activities influence F_{CO2}, but the effects seen here were different depending on the kind of activities. Weeding and crop harvesting always led to an increase in the CO_2 absorption rate after a short-time decrease (the 3rd, 6th, and 7th shaded bars in Fig. 3), because the thinning of herbaceous plant stimulated a new, rapid growth of the herbaceous species. Preparation activities (including land smoothing, fertilization, and irrigation) in the first month of a crop term always led to an emission of CO_2, because GEP was decreased in a time when ER was not noticeably changed (the 5th and 6th shaded bars in Fig. 3b–d).

Inundation led to a significant decrease in GEP and ER, and turned F_{CO2} to positive when WT was high (the 4th shaded bar in Fig. 3). With WT falling, F_{CO2} turned to negative since GEP values were increasing with the number of leaves exposed, while the ER values remained low. Once the flood was settled, there was an eruption of CO_2 within a short time period because of the sharp increase of ER induced by the significant increase of T_s.

ER showed strong seasonality during the three years while GEP varied with the dynamic of NDVI. The maximum GEP in the three years was 1881 (May 6th), 860 (July 4th), and 1102 (June 8th) mmol m^{-2} d^{-1}, whereas the highest ER was 909 (July 29th), 691 (July 3rd), and 747 (July 31st) mmol m^{-2} d^{-1}, respectively. F_{CO2} did not show obvious seasonality during the three years. The largest absorption in 2012 (−462 on June 14th) and 2013 (−476 mmol m^{-2} d^{-1} on November 4th) both appeared when the crops were in a fast growing period, which was only a third of the largest absorption in 2011 (−1315 mmol m^{-2} d^{-1} on May 6th).

3.4. F_{CH4} dynamic

F_{CH4} values were small except during inundation (Fig. 3e). There was a flush of CH_4 during inundation, with a maximum daily F_{CH4} of ~4000 μmol m^{-2} d^{-1}. Notably, two peaks appeared on July 16th (4278.5 μmol m^{-2} d^{-1}) and August 12th (4394.4 μmol m^{-2} d^{-1}), 2012, and the lowest F_{CH4} appeared on July 23rd, 2012 when the WT was ~2.5 m. In non-inundated months, F_{CH4} fluctuated slightly around zero, with an average of 1.62 ± 0.41 nmol m^{-2} s^{-1} and a maximum emission (absorption) rate of 249.38 ± 32.32 (−302.42 ± 37.80) nmol m^{-2} s^{-1}.

At a monthly scale, the cutover remained a weaker sink of CH_4 in the first three months after the clear-cutting (July–September, 2011), but turned to a net source in the fourth month (October 2011) (Fig. 4b). The monthly uptake of CH_4 before the clear-cutting varied from −0.3 ± 0.1 mmol m^{-2} (April) to −4.6 ± 2.3 mmol m^{-2} (July), but declined to −1.4 ± 0.4 mmol m^{-2} in July–September. In inundation months, the monthly F_{CH4} was 42.9 ± 7.7 and 64.4 ± 8.3 mmol m^{-2} in July and August, respectively, constituting 83.8% of annual emission (128.0 ± 42.4 mmol m^{-2}). In the non-inundation months since October 2011, the average monthly F_{CH4} was 3.3 ± 1.0 mmol m^{-2}, with a maximum of 7.3 ± 5.8 mmol m^{-2} (June 2013). Interestingly, there was a small absorption in July (−0.4 ± 5.6 mmol m^{-2}) and November (−0.1 ± 3.2 mmol m^{-2}) of 2013, which was consistent with the fact that the field was a CH_4 sink in the fast growing season of 2011 and a weak source in the non-growing season of 2012.

3.5. Harvest and intercropping effects on total carbon fluxes

Clear-cutting significantly reduced CO_2 absorption in the following two years, according to the fluxes in the first six months of years (Fig. 5a). F_{CO2} in 2012 and 2013 decreased to 8.7% and 30.5% of that in 2011, respectively. F_{CO2}, prior to the clear-cutting, was significantly ($p < 0.05$) higher than that in the young plantation in the first year. The GEP in 2012 and 2013 decreased to 47.0% and 67.2% of that in 2011, while ER was 84.4% and 103.1%, respectively. Additionally, the mean air temperature in January–June 2011 and 2012 remained at the same level (14.02 and 13.93 °C, respectively), while mean soil temperature differed by ~2 °C (12.33 and 14.30 °C, respectively). On the contrary, the clear-cutting elevated ecosystem CH_4 emission. According to the filled data in the first six months of a year, CH_4 emission in 2012 and 2013 was 3.5 and 11.4 times of that in 2011, respectively (Fig. 5a). More persuasively, F_{CH4} in April–June 2013 was 17.19 μmol m^{-2} while it was −3.45 μmol m^{-2} in 2011.

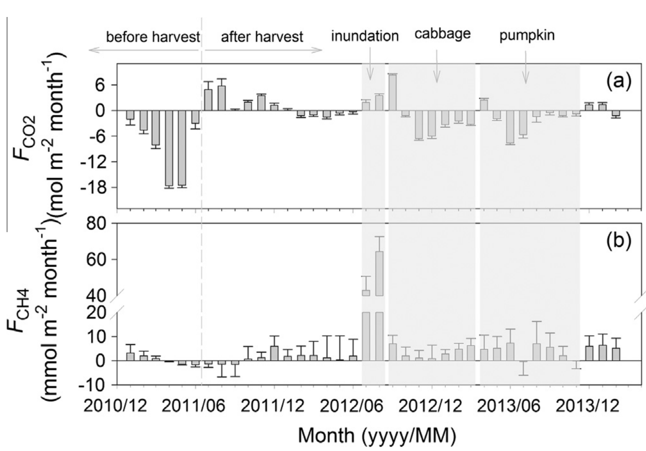

Fig. 4. Monthly fluxes of: (a) CO_2 (F_{CO2}) and (b) CH_4 (F_{CH4}). The error bars are the 95% confidence intervals (CI).

From October to next February, intercropping of cabbage had minor effect on F_{CH4}, but turned the field from a weak CO_2 source to a strong sink (Fig. 5c). F_{CH4} in the three periods was not significantly different from each other, although the F_{CH4} in the third period (19.6 mmol m^{-2}) was slightly larger than the first two periods (11.9 and 11.7 mmol m^{-2}, respectively). However, the uptake of CO_2 (−19.5 mol m^{-2}) in the months with cabbage intercropping was significantly ($p < 0.05$) higher than that without intercropping (5.5 and −0.41 mol m^{-2}), because GEP was larger while ER was slightly smaller in comparison to those of the other two periods. In addition, both F_{CH4} and F_{CO2} were not significantly different in the periods of cabbage and pumpkin intercropping (Fig. 5d), though ER and GEP during pumpkin intercropping were both significantly ($p < 0.01$) larger than that during cabbage cultivation.

3.6. Inundation effects on F_{CH4}

Inundation significantly increased CH_4 emission. F_{CH4} in July and August of 2012 (107.3 mmol m^{-2}) was −134.0 and 15.2 times higher than those of 2011 and 2013, respectively (Fig. 5b). When WT was below −1.0 m of the ground, F_{CH4} was small and did not obviously vary with WT (Fig. 6). However, when WT rose from −1.0 m to the ground, F_{CH4} increased slightly, inferring that trapped CH_4 in the soil was extruded out by the rising WT. When WT was above ground, F_{CH4} increased dramatically with WT and reached a high level when WT was 0.5–1.5 m.

The relationship between WT and half-hourly F_{CH4} and between WT and class-averaged F_{CH4} (filled and un-filled) in 2012 was simulated with the following equation:

$$Y = a \cdot EXP\left(-0.5\left(\frac{X - X_0}{b}\right)^2\right) \quad (1)$$

where Y is half-hourly F_{CH4}; X is WT; a, b and X_0 are three parameters; and a is the maximum $F_{CH4,}$ and X_0 is the WT where F_{CH4} reaches the maximum. The F_{CH4} is supposed to reach the maximum of ~40 nmol m^{-2} s^{-1} when WT is ~1.2 m (Table 1).

3.7. Environmental controls on F_{CH4}

Regulations of half-hourly F_{CH4} seemed complicated. The empirically-selected variables can significantly interpret the half-hourly F_{CH4} in 32 weeks, but only accounted for 11.3% ± 9.3% (mean ± SD) of the total variation (Appendix B). Nevertheless, U_{star} and R_n were the most frequent explanatory variables, both appearing for 9 weeks. Moreover, U_{star} always appeared in weeks after a heavy rain or with continuously light rainfall or during inundation, while R_n always appeared in cloudy or rainy weeks during October–February. In addition, WT and VWC were the most significant variables regulating daily and weekly F_{CH4}. At a daily-to-seasonal scale, WT or VWC significantly explained 6 of 10 seasons alone or with one other variable (Table 2). At a daily-to-yearly scale, VWC or/and WT explained flux in 2011, 2012, and 2011–2014. At a weekly-to-yearly scale, WT and VWC interpreted all the years except 2013.

3.8. Net carbon budget and GHG flux

Our site was a net carbon sink in the harvest year and during the first two years of the new plantation (Table 3). The net carbon

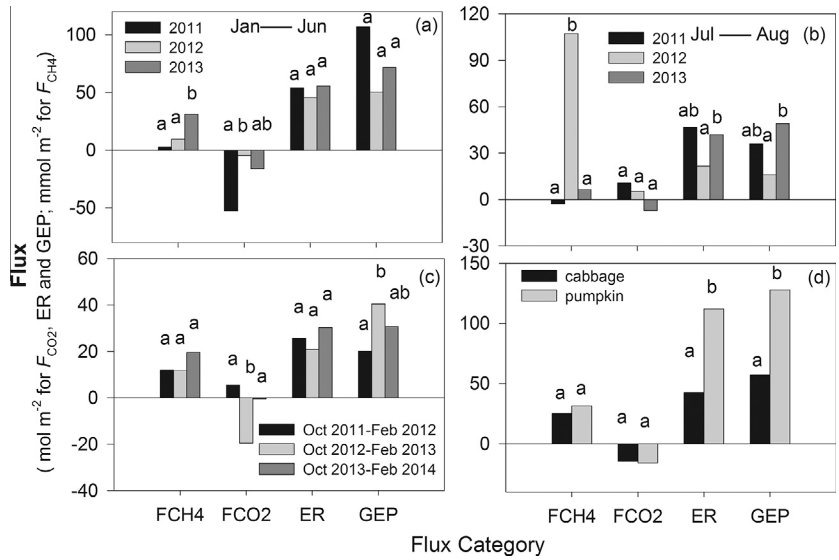

Fig. 5. Comparison of F_{CH4}, F_{CO2}, ecosystem respiration (ER), and gross ecosystem production (GEP) in different periods, including (a) from January to June in different years, (b) July and August in different years, (c) from October to the next February in different years, and (d) cabbage (September 2012–March 2013) and pumpkin (April–October 2013) cultivation period. Two-sample *T*-test for Means was used to determine the significant difference between different periods. Without the same character above, the two bars in one group indicate significant the difference ($p < 0.05$) to each other.

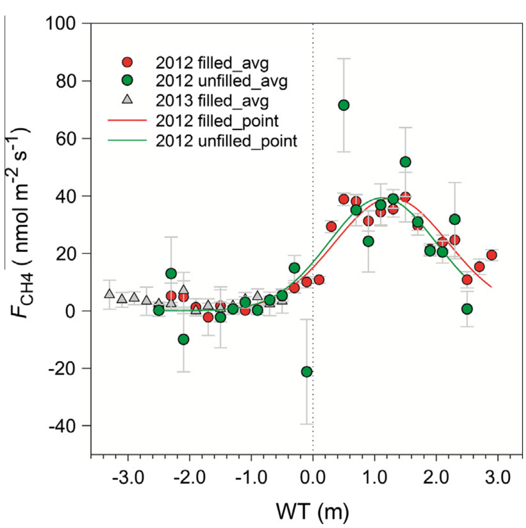

Fig. 6. Variability of F_{CH4} with ground water table (WT). The half-hourly F_{CH4} was partitioned into different classes by WT, which was graded by 0.2 m. The bar indicates one time of standard error (±SE). The trend lines are for the gap-filled and unfilled half-hourly fluxes with Eq. (1) (see Table 1 for more explanations).

Table 1
The results of modeling the relationship between F_{CH4} and WT with Eq. (1). The datasets with _avg are the average half-hourly F_{CH4} in different WT classes, while those with _point are the half-hourly F_{CH4}. WT was divided into 0.2-m classes.

Dataset	*a*	*b*	X_0	R^2	*F*	*p*
Filled_point	39.25*	0.92*	1.27*	0.11	371.9	<0.0001
Unfilled_point	39.35*	0.87*	1.13*	0.09	98.0	<0.0001
Filled_avg	39.13*	0.92*	1.27*	0.71	148.3	<0.0001
Unfilled_avg	37.38*	0.92*	1.17*	0.57	47.0	<0.0001

* $p < 0.0001$.

budget in the 2011 harvest year (-424.3 ± 52.5 g-C m^{-2}) was the largest of the three, but the mature plantation (January–June 2012) absorbed -633.5 ± 28.3 g-C m^{-2} (including both CH_4 and CO_2). This suggests that the cutover (July–December 2012) was a net carbon source (209.2 ± 31.4 g-C m^{-2}) (Fig. 4a). However, it turned into a carbon sink at the beginning of the first growing season following the harvest, resulting in an annual carbon budget after clear-cutting (July 2011–June 2012) of 154.1 ± 83.2 g-C m^{-2} (Table 3). The emission (165.1 ± 9.6 g-C m^{-2}) in the months of inundation (July–August 2012) and soil preparation for cabbage cultivation (September 2012) was offset by the uptake (-165.1 ± 8.9 g-C m^{-2}) during cabbage growing during October–December 2012. In the second year after the clear-cutting, the field was a net carbon sink in every month except April (i.e., the preparing month from pumpkin cultivation) and December. Carbon emission in CH_4 offset 0.018%, 2.78%, and 0.21% of carbon uptake in CO_2 in 2011–2013, respectively. In addition, the field was a net sink of GHG in each year (Table 3). The contribution of $F_{CH4\text{-}CO2eq}$ was 0.04 ± 0.03, 3.58 ± 1.19, and 1.44 ± 0.81 mol-CO_2_eq m^{-2}, which offset 0.50%, 77.96%, and 5.93% of GHG uptake in CO_2 of the three years, respectively.

4. Discussion

4.1. Clear-cutting effects on carbon fluxes

Clear-cutting effects on ecosystem carbon budget vary by climatic regions. In the boreal forests of Canada, the CO_2 emission in the first year after clear-cutting ranged from ~200 to ~600 g-C m^{-2} yr^{-1} (Howard et al., 2004; Humphreys et al., 2005; Machimura et al., 2005; Zha et al., 2009); it took ~10 years before it turned back into a net sink of CO_2 (Fredeen et al., 2007; Howard et al., 2004; Kurz and Apps, 1994; Zha et al., 2009). Similarly in Finland, the 4-year-old stand after clear-cutting was still a source of carbon throughout the year (386 g-C m^{-2} yr^{-1}), while the 12-year-old stand was nearly neutral (Kolari et al., 2004). In a cool-temperature mixed forest in Japan, the CO_2 emission in the first year after clear-cutting was 569 g-C m^{-2} yr^{-1}, and ~7 years later the clearcut regained as a carbon sink (Aguilos et al., 2014; Takagi et al., 2009). In a slash pine plantation forests in North Florida, USA with warm and humid climate, the CO_2 emission during the first year following the harvest ranged from 742 to 1269 g-C m^{-2} yr^{-1} (Clark et al., 2004; Gholz and Fisher, 1982), and turned neutral after ~3 years (Gholz and Fisher, 1982). In contrast, the effect of clear-cutting on ecosystem carbon balance at our site was much weaker. The overall CO_2 emission was only 209 g-C m^{-2} (July–January) before it turned back to be a net carbon sink

Table 2
Regression models for daily and weekly mean F_{CH4} (μmol m^{-2} d^{-1}) by stepwise linear regression method. Soil temperature (T_s), water table (WT), soil volumetric water content (VWC), normalized difference of vegetation index (NDVI), logarithmic transformed GEP (LnGEP), friction velocity (U_{star}), and vapor pressure deficit (VPD) were involved at the beginning of stepwise regression.

Periods	Model (Ln(F_{CH4} + 10)=)	R^2	$p > F$	RMSE	n
Daily to seasonal/annual					
Natural seasons					
10/11–11/11	$-25.5 + 0.65 \times U_{star} + 136.2 \times VWC - 166.9 \times VWC^2$	0.29	0.0003	0.20	59
	$-24.07 + 129.74 \times VWC - 159.17 \times VWC^2$	0.21[b]	0.0011	0.21	61
12/11–02/12	$1.43 + 0.34 \times T_s - 0.02 \times T_s^2 - 0.036 \times WT^2$	0.40	<.0001	0.09	80
	$6.95–20.21 \times VWC + 22.13 \times VWC^2$	0.21[b]	<.0001	0.17	91
03/12–05/12	$1.96–0.038 \times WT^2 + 1.67 \times VWC$	0.75	0.0005	0.03	25
06/12–08/12[a]	$4.42–3.75 \times NDVI$	0.44	<.0001	0.74	46
	$0.72 + 0.34 \times WT + 6.71 \times VWC^2$	0.44[b]	<.0001	0.68	62
09/12–11/12	$3.89–0.19 \times T_s + 0.005 \times Ts^2$	0.24	<.0001	0.23	90
	$2.85 + 0.51 \times WT + 0.12 \times WT^2$	0.16[b]	0.0005	0.25	91
12/12–02/13	$6.70 + 2.30 \times WT + 0.30 \times WT^2 - 0.80 \times 10^{-3} \times VPD^2$	0.47	<.0001	0.07	84
	$6.67 + 2.30 \times WT + 0.30 \times WT^2$	0.39[b]	<.0001	0.07	90
03/13–05/13	$2.26 + 0.056 * VPD - 0.002 * VPD^2$	0.24	<.0001	0.26	42
06/13–08/13	$2.63–0.74 \times 10^{-3} \times VPD^2$	0.15	0.0047	0.34	52
09/13–11/13	$0.85 + 0.076 \times WT^2 + 2.48 \times NDVI^2$	0.24	<.0001	0.24	80
12/13–02/14	$2.38 + 1.30 \times VWC - 0.0051 \times (LnGEP)^2$	0.23	0.0001	0.07	73
Years					
2011(10–12)	$3.25 + 0.46 \times U_{star} - 6.09 \times VWC^2$	0.26	<.0001	0.19	79
2012[a]	$3.48–6.83 \times VWC^2$	0.27	<.0001	0.19	235
2013	$6.93 + 0.21 \times WT + 0.046 \times WT^2 - 19.04 \times VWC + 21.52 \times VWC^2 - 1.32 \times NDVI^2$	0.47	<.0001	0.38	275
2014(01–02)	$2.85 + 0.39 \times WT + 0.07 \times WT^2$	0.40	<.0001	0.39	49
2011–2014	$2.48–4.98 \times 10^{-3} \times VPD$	0.02	0.0148	0.26	638
Weekly to annual					
2011	$-560.59–412.60WT - 75.71WT^2$	0.74	0.0003	0.35	15
2012[a]	$0.33 + 7.01 \times VWC^2 + 5.06 \times U_{star}^2 - 4.61 \times NDVI^2$	0.75	<.0001	0.39	41
2013	$1.63–1.59 \times U_{star}^2$	0.09	0.0407	0.35	45
2014	$1.38–1.46 \times U_{star} + 1.57 \times VWC$	0.92	0.0017	0.05	8
2011–2014	$2.27 + 0.47 \times WT + 0.08 \times WT^2 - 0.78 \times NDVI^2$	0.47	<.0001	0.39	105

[a] Indicates a period with inundation.
[b] Indicates that the model is built with a stepwise regression method including WT, WT^2, VWC, and VWC^2 only as initial variables.

Table 3
Annual and overall F_{CH4}, F_{CO2}, GEP, ER, GHG fluxes, and carbon budget. MDV indicates the gaps of F_{CH4} were filled with gliding-window mean diurnal variations method. MI indicates the gaps of F_{CH4} and F_{CO2} were filled with multiple imputation method; NLR indicates the gaps of F_{CO2} were filled with a nonlinear regression method. GHGs flux is the sum of F_{CO2} and 28 times of F_{CH4}. A 95% confidence interval (95% CI) was derived from MI except the F_{CH4} in 2011, which was propagated from monthly uncertainty. A 95% CI of GHG flux and carbon budget was propagated from the uncertainty of F_{CH4} and F_{CO2}.

Year	F_{CH4} (mmol m^{-2})				F_{CO2} (mol m^{-2})			GEP	ER	GHG flux (mol-CO$_2$_eq m^{-2})		Carbon budget (g-C m^{-2})	
	MDV	Unfilled	MI	95% CI	NLR	MI	95% CI	(mol m^{-2})			95% CI		95% CI
2011	6.3	9.5	−1.4	11.1	−35.4	−32.8	4.4	168.3	133.0	−35.2	4.4	−424.3	52.5
2012	128.0	157.7	137.9	42.4	−4.6	−7.3	1.9	101.0	96.4	−1.0	2.2	−53.6	22.8
2013	51.5	33.0	45.4	29.1	−24.3	−18.9	2.9	160.1	135.9	−22.8	3.0	−290.7	34.2
P0[a]	11.8	24.6	19.9	19.8	12.8	−20.6	6.9	111.7	124.6	13.2	67.0	154.1	83.2
Total	185.8	200.3	181.9	52.6	−64.2	−59.0	5.6	429.5	365.2	−59.0	5.8	−768.6	66.7

[a] 1-year period after clear-cutting (July 1st, 2011–June 30th, 2012).

on the arrival of next growing season. In the first 1-year period post clear-cutting (July 2011–June 2012), the GEP of the cutover was 1341 g-C m^{-2} yr^{-1} (Table 3), which was much larger than those from the Douglas-fir cutovers in Canada (130–220 g-C m^{-2} yr^{-1}) (Humphreys et al., 2005; Paul-Limoges et al., 2015), the cool-temperate mixed forest cutover in Japan (481 g-C m^{-2} yr^{-1}) (Aguilos et al., 2014; Takagi et al., 2009) and the pine plantation cutovers in Florida (705 g-C m^{-2} yr^{-1}) (Clark et al., 2004). The GEP was nearly all from the understory species for the tree leaves was underdeveloped. On the other hand, the ER from the cutover at our site was 1495 g-C m^{-2} yr^{-1} in the same period (July 2011–June 2012), which was larger than that from the Douglas-fir cutovers (840–1130 g-C m^{-2} yr^{-1}) (Humphreys et al., 2005; Paul-Limoges et al., 2015), but similar with that from the cool-temperate mixed forest cutover (1395 g-C m^{-2} yr^{-1}) (Aguilos et al., 2014; Takagi et al., 2009), and slight smaller than that from the pine plantation cutovers (1974 g-C m^{-2} yr^{-1}) (Clark et al., 2004). Thus, we conclude that the high productivity of understory vegetation was the changed primary component responsible for the low carbon emission induced by the clear-cutting at our site. In fact, the abundant and fast growing understory species always weaken the emission induced by clear-cutting and shorten the term of carbon source after clear-cutting (Kowalski et al., 2003; Machimura et al., 2005; Takagi et al., 2009).

Clear-cutting effect on ER appeared less drastic than that on GEP (Clark et al., 2004; Humphreys et al., 2005; Takagi et al., 2009). Nevertheless, the living biomass removal and residual biomass (e.g. stump) retention would change the composition of ER. Paul-Limoges et al. (2015) reported that ER decreased by 15% in the first year after clear-cutting of a Douglas-fir forest, inferring that a significant reduction in autotrophic component of ER in the post-harvest stand was compensated by increased heterotrophic respiration as a result of decomposition of logging residue. Similarly, Noormets et al. (2012) revealed that a 60% increase in heterotrophic respiration induced by the pulse of detritus produced at harvest of loblolly pine plantation in North Carolina that was offset by the decrease in autotrophic respiration, resulting in little change of ER. Williams et al. (2014) showed that coarse woody debris at a temperate, deciduous broadleaf forest clearcut contributed 18% of daytime ER during summer months in the first three years. At our site, the ER in the first January–June after clear-cutting just decreased by 15.6% (Fig. 5a, Section 3.5). In addition, according to previous studies at our site (Han, 2008; Zhang, 2013), the soil respiration (R_s) in April 2012–March 2013 (P1, 1-year stand, 1147 g-C m^{-2} yr^{-1}) was nearly the same with that in July 2005–June 2007 (P2, 6- and 7-year old stand, 1148 g-C m^{-2} yr^{-1} in average) (Table 4). However, the ER in P1 (1220.9 g-C m^{-2} yr^{-1}) was 16.3% lower than that in P2 (1459.2 g-C m^{-2} yr^{-1}). It means that the aboveground respiration (R_{AG}, including aboveground living biomass respiration and aboveground woody detritus decomposition) in P1 (73.9 g-C m^{-2} yr^{-1}) constituted only 6.0% of ER and was 23.7% of that in P2 (311.2 g-C m^{-2} yr^{-1}). The ratio of R_s to ER (94.0%) was similar to that (~100%) at the cool-temperature mixed forest clearcut in the first year (Takagi et al., 2009). Moreover, the soil heterotrophic respiration (R_{SH}, not including the decomposition of freshly dead residual root during observation) in P1 (748.2 g-C m^{-2} yr^{-1}) was 61.3% of ER and was higher than that in P2 (598.5 g-C m^{-2} yr^{-1}), may due to the decomposition of the larger amount of dead, fine root in the soil as well as the increased soil temperature (16.60 and 15.57 °C, respectively, and July 11th–August 20th was not included in each period); Meanwhile, the root respiration (R_{ROOT}), including living root respiration and freshly dead residual root decomposition) in P1 (398.8 g-C m^{-2} yr^{-1}) was only 32.7% of ER and 72.5% of that in P2 (550.3 g-C m^{-2} yr^{-1}). Therefore, compared to P2, it seemed that: (1) ER decreased by 16.3% after clear-cutting due to the dramatic decline in aboveground respiration and slight decrease in root respiration, as well as the compensation by the increased R_{SH}; (2) clear-cutting effect on R_{ROOT} was not as drastic as that on aboveground biomass respiration, likely because of the fast developing living root of understory vegetation and the fact that the residual roots main remained alive for the first few years (Noormets et al., 2012); (3) the contribution of the root-free parts (e.g., aboveground materials) of the stump to ER was small (this contributed only 6% together with above ground biomass). According to the finding of meta-analysis by Subke et al. (2006), the ratio of R_{SH} to R_S would consistently decline, resulting in a consistent increase of the ratio of autotrophic respiration to ER. Therefore, the aforementioned inferences were also defensible when regarding to the mature stand. However, several years after clear-cutting, amount of live roots would be minimal while decomposition of large coarse woody debris continue their contributions to ER (Noormets et al., 2012).

Several studies reported that clear-cutting decreased the CH_4 uptake and even turned the field into a CH_4 source in a short term (Gundersen et al., 2012; Lindroth et al., 2012; Sun et al., 2011; Sundqvist et al., 2014). At our site, the absorption of CH_4 was only 20–30% of that in an undisturbed stand in the first two months after clear-cutting (Gao et al., 2013). However, several months later, the field turned into a CH_4 source. At this site, WT, VWC, and U_{star} were supposed to be the most important regulators on F_{CH4}. We infer that clear-cutting effects on F_{CH4} were primarily modulated by the three environmental factors. On one hand, clear-cutting elevated WT (Dubé et al., 1995), thus the depth from the hotspot to the soil surface was shortened and the opportunity of CH_4 oxidation decreased. On the other hand, the removal of trees greatly decreased the roughness length, thereby increasing the turbulence near the soil surface that accelerated the transfer of CH_4 from soil to atmosphere (Chu et al., 2014). Additionally, the removal of trees would decrease the transpiration from the deep soil, resulting in a relative higher soil moisture that promotes CH_4 production (Castro et al., 2000; Wu et al., 2011). The harvest residue effect on F_{CH4} was not examined at our site although previous studies indicated that stump removal did not have significant effects on CH_4 flux (Kataja-aho et al., 2012; Sundqvist et al., 2014) and aboveground logging residue had no change on F_{CH4} (Mäkiranta et al., 2012).

Table 4
Components of ER of the clearcut and the mid-age stand. Trench method was used to separate the soil respiration (R_S) into root-derived soil respiration (R_{ROOT}) and soil heterotrophic respiration (R_{SH}). The aboveground respiration (R_{AG}) was ER minus R_S. After clear-cutting (P1), R_{ROOT} included aboveground plantation respiration and aboveground coarse woody residue (e.g. aboveground part of the stumps) decomposition, while R_{ROOT} included the living roots respiration and decomposition of freshly dead root during P1. The units are g-C m^{-2} yr^{-1}.

Period	ER	R_S	R_{AG}	R_{ROOT}	R_{SH}	Reference
April 2012–March 2013 (P1)	1220.9	1147.0	73.9	398.8	748.2	zhang (2013)
July 2005–June 2007 (P2)	1459.2	1148.7	310.5	550.3	598.5	–
July 2005–June 2006	1389.1	1066.6	322.5	532.0	534.6	Han (2008)
July 2006–June 2007	1529.2	1230.8	298.4	568.5	662.3	Han (2008)

4.2. WT effects on F_{CH4}

WT and VWC were supposed to be important controls on daily and weekly F_{CH4}. In fact, inundation has significant influence on many geochemical processes (Krause et al., 2007). When WT is below ground, it determines the border of the aerobic and anaerobic region of soil or water, where is the hotspot for GHG losses (Krause et al., 2007). When WT was lower, the CH_4 produced at this hotspot has to pass through a longer distance in an aerobic region before discharging to the atmosphere, thus more CH_4 will be oxidized (Bridgham et al., 2013). This supports the fact that monthly CH_4 emission decreased gradually from late summer to winter in 2012 and 2013 (Fig. 4b). However, soil water can hinder CH_4 transfers from the hotspot to the soil surface (Sundqvist et al., 2014). When VWC is lower, the transfer of gas will be faster, suggesting that less amount of CH_4 will be oxidized before arriving at the soil surface. Thus, the difference in VWC might be the reason for the differences in F_{CH4} over the three winters (Figs. 2c and 4b). In addition to WT and VWC, U_{star} was another important factor on F_{CH4} in some non-growing seasons, indicating the importance of the turbulence mixing on increasing gas transfer speed (Chu et al., 2014). Thus, we infer that the new plantation will become a CH_4 sink in future non-inundation years when the WT is lower for the increasing transpiration, when VWC is higher, and when surface U_{star} is smaller for the coverage of herbage.

When WT is above ground, it increases the anaerobic layer that would benefit CH_4 production (Best and Jacobs, 1997; Grünfeld and Brix, 1999; Vann and Megonigal, 2003) and increases the resistance of CH_4 transfer (Ding et al., 2002; Zona et al., 2009). Thus, when WT is high enough, it will decrease CH_4 emission (Figs. 3e and 6). This may be one of the reasons why CH_4 emission rate from open water was lower than that from the drawdown area of the Yangtze River (Chen et al., 2011). Most studies revealed that the CH_4 emission rate was higher when inundation depth was shallow (2–15 cm) (Altor and Mitsch, 2006; Ding et al., 2002; Moore and Knowles, 1989; Ren et al., 2002). However, in this study, F_{CH4} reached the peak when inundation depth was ~1.2 m, likely because the flood flowed quickly and numerous eddies in the flow can bring up the bubbles with CH_4 from the deep water.

4.3. Magnitude of F_{CH4}

The floodplain of a large river experiences a wet and a dry period over the year. In the dry season, the soil is well aerated; therefore, the riparian ecosystems can oxidize CH_4 as upland grassland and forest ecosystems. This phenomenon has been reported in many studies (Hopfensperger et al., 2009; Sun et al., 2013b, 2013c) and was also seen at this site in the mature plantation and in the newly planted stand (Figs. 3e and 4b). As for CH_4 consumption, the mature plantation at this site was comparable with other forest ecosystems. Dalal et al. (2008) summarized that the maximum CH_4 consumption rate of forest was no higher than 0.15 mmol m^{-2} d^{-1}. Before clear-cutting, the mature plantation in fast growing months was a net CH_4 sink, with F_{CH4} ranged from −0.142 to 0.009 mmol m^{-2} d^{-1} (mean of −0.038 ± 0.034 mmol m^{-2} d^{-1}), which was close to that of sub/tropical forest in Australia (−0.036 ± 0.024 mmol m^{-2} d^{-1}) (Dalal et al., 2008) and slightly higher than that in a temperate forest of Beijing, China (−0.031 mmol m^{-2} d^{-1}) (Sun, 2000).

F_{CH4} at our site was very small in non-inundation periods comparing with the area on the upper and lower reaches of Yangtze River. The mean daily F_{CH4} in non-inundation months ranged from −0.012 to 0.24 mmol m^{-2} d^{-1}, with a mean of 0.11 ± 0.08 (mean ± SD) mmol m^{-2} d^{-1}, which was only a quarter of that in the drawdown area (0.44 mmol m^{-2} d^{-1}) on upper reaches (Chen et al., 2011) and was <1/30 of that in the estuary mash (3.09 mmol m^{-2} d^{-1}) of Yangtze River (Wang et al., 2009). However, during inundation months, the mean daily F_{CH4} ranged from 0.33 to 4.39 mmol m^{-2} d^{-1} with a mean of 2.17 ± 1.16 mmol m^{-2} d^{-1}. This was ~5 times of that (0.44 mmol m^{-2} d^{-1}) in drawdown area of the upper reaches of Yangtze River (Chen et al., 2011). Notably, the highest emission rate of CH_4 was slightly larger than the mean rate of the subtropical wetland in Australia (4.2 mmol m^{-2} d^{-1}) (Dalal et al., 2008), which means that the overall budget of CH_4 from the large area of the riparian zone in the middle and lower reaches of Yangtze River would vary in a wide range and differ between years depending on the inundation situation. This would enlarge the uncertainty in estimating global CH_4 balance. Nevertheless, CH_4 emission on the floodplain of the Yangtze River was much smaller than those on the forested floodplain of tropical rivers. F_{CH4} emissions in flooded forests on the floodplain of Amazon and Orinoco River were 12 ± 1.68 mmol m^{-2} d^{-1} (Bartlett et al., 1988) and 6.79 ± 36.2 mmol m^{-2} d^{-1} (Smith et al., 2000), which were 5.5 and 3.1 times that of this site during inundation, respectively.

Previous studies showed that carbon released in CH_4 contributed significantly to the overall wetland's GHG budget (Chu et al., 2014; Hatala et al., 2012; Herbst et al., 2011; Olson et al., 2013). At this site, GHG emission in CH_4 balanced out ~80% of GHG uptake in CO_2 in the inundation year after clear-cutting. However, this emission is only ~5% of annual GHG uptake in CO_2 (72.8 mol-CO_2 m^{-2}) of the immature plantation at this site (Xiao et al., 2013). This portion is much smaller than reported wetland ecosystems (Chu et al., 2014; Olson et al., 2013).

5. Conclusions

Clear-cutting of the poplar plantation on the floodplain turned the ecosystem from a strong carbon sink to a source only during the rest months of the same year the clear-cutting was made. The ecosystem turned to be a net carbon sink immediately upon the arrival of the following growing season because of the large productivity of understory species in this region. Clear-cutting turned the ecosystem from a CH_4 sink to a CH_4 source after the third month since the harvest. However, CH_4 emission only balanced out a very small portion of carbon sequestration in CO_2 during the three years. CH_4 emission in the non-inundated period was weak, but inundation induced a large amount of CH_4 emission, indicating the high probability of large inter-annual variation of CH_4 budget. Water table (WT), soil water content (VWC) and friction velocity (U_{star}) were the most significant regulators for F_{CH4} during non-inundation period, while inundated depth was the critical control on F_{CH4} during inundation. This highlights the importance of considering the Yangtze River's water level when estimating the regional CH_4 and GHG balance. This study indicates a large capacity of carbon sequestration in the whole cycle of poplar plantation in this region.

Acknowledgements

This site is supported by the US-China Carbon Consortium (USCCC). This research is funded by the National Science & Technology Pillar Program Projects (2015BAD07B04; 2015BAD07B07). Junshan District Bureau of Forestry and Ecology helped in station maintenance, Daoping Xiong helped in data collection; Gabriela Shirkey edited an early version of the manuscript.

Appendix A

The removed and residual biomass was calculated by the empirical models of Wu et al. (2001). Prior to the harvest, the averaged canopy height (H) was 19.5 m, the mean diameter at breast height (D) was 23 cm, and the stand density was ~500 trees per ha. The removed biomass consisted ~95% trunk, ~95% branch and ~50% foliage, while the residual biomass included 5% trunk and branch (aboveground), 50% foliage (aboveground), and 100% root (below ground).

The removed trunk was calculated as

$$0.025824 \times (D^2H)^{0.908408} \times 500 \times 95\% = 54.28 \text{ t ha}^{-1} \tag{A.1}$$

The removed branch was calculated as

$$0.0872504 \times (D^2H)^{0.627919} \times 500 \times 95\% = 13.73 \text{ t ha}^{-1} \tag{A.2}$$

The removed foliage was calculated as

$$0.0325842 \times (D^2H)^{0.585471} \times 500 \times 50\% = 1.82 \text{ t ha}^{-1} \tag{A.3}$$

Thus, the overall removed biomass was 69.83 t ha^{-1}.

The residual root was calculated as

$$0.0417555 \times (D^2H)^{0.697130} \times 500 \times 100\% = 13.11 \text{ t ha}^{-1} \tag{A.4}$$

The residual Trunk was calculated as

$$0.025824 \times (D^2H)^{0.908408} \times 500 \times 5\% = 2.86 \text{ t ha}^{-1} \tag{A.5}$$

The residual branch was calculated as

$$0.0872504 \times (D^2H)^{0.627919} \times 500 \times 5\% = 0.72 \text{ t ha}^{-1} \tag{A.6}$$

The residual foliage was calculated as

$$0.0325842 \times (D^2H)^{0.585471} \times 500 \times 50\% = 1.82 \text{ t ha}^{-1} \tag{A.7}$$

Thus, the overall residual biomass was estimated at 18.51 t ha^{-1} (where 13.11 t ha^{-1} was belowground and 5.40 t ha^{-1} was aboveground). The stump, including root and residual trunk, was 15.97 t ha^{-1}.

Appendix B

Regression models of F_{CH4} at half-hourly to weekly scale. Soil temperature (T_s), water table (WT), soil volumetric water content (VWC), friction velocity (U_{star}), logarithmic transformed GEP (LnGEP), net radiation (R_n), vapor pressure deficit (VPD), and ground heat flux (G) were involved at the initial stepwise regression.

Year	Week	Model ($\mathrm{Ln}(F_{CH4} + 400)$=)	R^2	$p > F$	RMSE	n
2011	40	$6.00 - 0.903 \times 10^{-3} \times \mathrm{VPD}$	0.266	0.0410	0.014	80
	41	$6.06 - 0.252 \times U_{star}$	0.050	0.0139	0.110	121
	42	$7.29 + 0.488 \times \mathrm{WT}$	0.036	0.0295	0.071	146
	43	$5.99 + 0.056 \times U_{star}$	0.037	0.0429	0.034	110
	44	$5.85 + 0.008 \times T_s$	0.056	0.0098	0.036	118
	45	$6.00 - 0.040 \times 10^{-3} \times R_n$	0.090	0.0088	0.017	75
	47	$5.97 + 0.120 \times U_{star}$	0.109	0.0001	0.033	130
	49	$5.99 + 0.073 \times 10^{-3} \times R_n$	0.149	0.0011	0.022	68
2012	1	$5.99 + 0.042 \times 10^{-3} \times R_n$	0.100	0.0012	0.014	102
	4	$5.97 + 0.004 \times T_s$	0.036	0.0393	0.018	118
	5	$5.99 + 0.050 \times 10^{-3} \times R_n$	0.056	0.0207	0.033	95
	24	$5.90 + 0.351 \times U_{star}$	0.067	0.0338	0.148	70
	27	$5.90 + 0.006 \times \mathrm{LnGEP}$	0.047	0.0029	0.016	188
	30	$7.67 - 0.706 \times \mathrm{WT}$	0.141	0.0079	0.148	50
	31	$6.070 - 0.096 \times U_{star}$	0.167	0.0040	0.026	50
	32	$6.25 - 0.109 \times \mathrm{WT} + 0.002 \times \mathrm{VPD} - 0.019 \times \mathrm{LnGEP}$	0.455	<.0001	0.039	120
	33	$-8.29 + 0.271 \times \mathrm{WT} + 11.134 \times \mathrm{VWC} + 0.071 \times U_{star}$	0.348	<.0001	0.031	183
	34	$6.01 + 0.016 \times \mathrm{LnGEP}$	0.034	0.0128	0.052	183
	42	$6.00 - 0.558 \times 10^{-3} \times G$	0.047	0.0321	0.041	98
	43	$5.99 + 0.074 \times U_{star} - 0.007 \times \mathrm{LnGEP}$	0.107	0.0374	0.030	92
	46	$5.98 - 0.124 \times 10^{-3} \times R_n$	0.166	0.0050	0.032	50
	47	$4.83 + 2.197 \times \mathrm{VWC}$	0.084	0.0073	0.031	84
2013	2	$5.99 + 0.030 \times U_{star}$	0.058	0.0193	0.019	94
	6	$6.74 - 1.466 \times \mathrm{VWC} - 0.037 \times 10^{-3} \times R_n$	0.129	0.0030	0.020	142
	7	$6.01 - 0.002 \times T_s$	0.052	0.0386	0.012	82
	8	$5.53 + 0.912 \times \mathrm{VWC} - 0.002 \times \mathrm{VPD}$	0.169	<.0001	0.014	109
	9	$6.00 + 0.019 \times 10^{-3} \times R_n$	0.042	0.0361	0.017	104
	11	$5.99 + 0.030 \times 10^{-3} \times R_n$	0.084	0.0059	0.020	89
	13	$5.98 + 0.049 \times U_{star} - 0.004 \times \mathrm{LnGEP}$	0.111	0.0042	0.021	96
	41	$6.06 + 0.360 \times 10^{-3} \times R_n - 0.076 \times \mathrm{LnGEP}$	0.141	0.0207	0.111	103
	45	$6.01 - 0.009 \times \mathrm{LnGEP}$	0.062	0.0111	0.029	104
	51	$5.98 - 0.003 \times G$	0.127	0.0358	0.028	50

References

Aguilos, M. et al., 2014. Dynamics of ecosystem carbon balance recovering from a clear-cutting in a cool-temperate forest. Agric. For. Meteorol. 197, 26–39. http://dx.doi.org/10.1016/j.agrformet.2014.06.002.

Altor, A.E., Mitsch, W.J., 2006. Methane flux from created riparian marshes: relationship to intermittent versus continuous inundation and emergent macrophytes. Ecol. Eng. 28 (3), 224–234.

Amiro, B.D. et al., 2010. Ecosystem carbon dioxide fluxes after disturbance in forests of North America. J. Geophys. Res.: Biogeosci. 115 (G4), G00K02. http://dx.doi.org/10.1029/2010JG001390.

Bartlett, K.B. et al., 1988. Methane flux from the central Amazonian floodplain. J. Geophys. Res.: Atmos. (1984–2012) 93 (D2), 1571–1582.

Best, E.P., Jacobs, F., 1997. The influence of raised water table levels on carbon dioxide and methane production in ditch-dissected peat grasslands in the Netherlands. Ecol. Eng. 8 (2), 129–144.

Bridgham, S.D., Cadillo Quiroz, H., Keller, J.K., Zhuang, Q., 2013. Methane emissions from wetlands: biogeochemical, microbial, and modeling perspectives from local to global scales. Global Change Biol. http://dx.doi.org/10.1111/gcb.12131.

Cannell, M., Milne, R., 1995. Carbon pools and sequestration in forest ecosystems in Britain. Forestry 68 (4), 361–378.

Castro, M.S., Gholz, H.L., Clark, K.L., Steudler, P.A., 2000. Effects of forest harvesting on soil methane fluxes in Florida slash pine plantations. Canadian J. For. Res. 30 (10), 1534–1542. http://dx.doi.org/10.1139/cjfr-30-10-1534.

Chen, J., 1996. Riparian vegetation characteristics and their functions in ecosystems and landscapes. Chinese J. Appl. Ecol. 7 (4), 439–448.

Chen, J. et al., 2004. Net ecosystem exchanges of carbon, water, and energy in young and old-growth Douglas-fir forests. Ecosystems 7 (5), 534–544.

Chen, H. et al., 2011. Methane emissions from the surface of the Three Gorges Reservoir. J. Geophys. Res. 116 (D21). http://dx.doi.org/10.1029/2011JD016244.

Chen, J. et al., 2014. Carbon fluxes and storages in forests and landscapes. In: Azevedo, J.C., Perera, A., Pinto, M.A. (Eds.), Forest Landscapes and Global Change: Challenges for Research and Management. Springer, pp. 139–166.

Chu, H. et al., 2014. Net ecosystem methane and carbon dioxide exchanges in a Lake Erie coastal marsh and a nearby cropland. J. Geophys. Res. 119, 722–740. http://dx.doi.org/10.1002/2013JG002520.

Clark, K.L., Gholz, H.L., Castro, M.S., 2004. Carbon dynamics along a chronosequence of slash pine plantations in north Florida. Ecol. Appl. 14 (4), 1154–1171.

Coaloa, D., Nervo, G., 2011. Poplar Wood Production in Europe on Account of Market Criticalities and Agricultural, Forestry and Energy Policy. Tercer Congreso Internacional de Salicáceas en Argentina.

Dalal, R.C., Allen, D.E., Livesley, S.J., Richards, G., 2008. Magnitude and biophysical regulators of methane emission and consumption in the Australian agricultural, forest, and submerged landscapes: a review. Plant Soil 309 (1–2), 43–76.

Ding, W., Cai, Z., Tsuruta, H., Li, X., 2002. Effect of standing water depth on methane emissions from freshwater marshes in northeast China. Atmos. Environ. 36 (33), 5149–5157.

Dinsmore, K.J., Skiba, U.M., Billett, M.F., Rees, R.M., Drewer, J., 2009. Spatial and temporal variability in CH_4 and N_2O fluxes from a Scottish ombrotrophic peatland: implications for modelling and up-scaling. Soil Biol. Biochem. 41 (6), 1315–1323.

Dubé, S., Plamondon, A.P., Rothwell, R.L., 1995. Watering up after clear-cutting on forested wetlands of the St. Lawrence lowland. Water Resour. Res. 31 (7), 1741–1750.

Falge, E. et al., 2001. Gap filling strategies for defensible annual sums of net ecosystem exchange. Agric. For. Meteorol. 107 (1), 43–69. http://dx.doi.org/10.1016/S0168-1923(00)00225-2.

Fredeen, A.L., Waughtal, J.D., Pypker, T.G., 2007. When do replanted sub-boreal clearcuts become net sinks for CO_2? For. Ecol. Manage. 239 (1), 210–216.

Gao, S. et al., 2013. Short-term effects of clear-cutting of *Populus deltoides* plantation on methane flux on the beach land of Yangtze River. Sci. Silvae Sin. 49 (1), 7–13.

Gao, S., Zhang, X., Tang, Y., Chen, J., Tang, J., Sun, Q., Tang, X., 2015. Dynamics and regulation of CH_4 fluxes in a poplar plantation on a floodplain. Acta Ecologica Sinica. http://dx.doi.org/10.5846/stxb201503220546.

Gholz, H.L., Fisher, R.F., 1982. Organic matter production and distribution in slash pine (*Pinus elliottii*) plantations. Ecology, 1827–1839.

Grünfeld, S., Brix, H., 1999. Methanogenesis and methane emissions: effects of water table, substrate type and presence of *Phragmites australis*. Aquat. Botany 64 (1), 63–75.

Gundersen, P. et al., 2012. The greenhouse gas exchange responses of methane and nitrous oxide to forest change in Europe. Biogeosci. Discussions 9 (5), 6129–6168.

Guo, J. et al., 2010. Effects of clear-cutting and slash burning on soil respiration in Chinese fir and evergreen broadleaved forests in mid-subtropical China. Plant Soil 333 (1–2), 249–261.
Hagedorn, F., Bellamy, P., 2011. Hot spots and hot moments for greenhouse gas emissions from soils. Soil Carbon Sensitive Eur. Ecosyst. 9–14. http://dx.doi.org/10.1002/9781119970255.ch2.
Han, S., 2008. Productivity Estimation of the Poplar Plantation on the Beaches in Middle and Lower Reaches of Yangtze River Using Eddy Covariance Measurement. Chinese Academy of Forestry, Beijing.
Hartmann, D.L. et al., 2013. Observations: atmosphere and surface. In: Stocker, T.F., Qin, D., Plattner, G.-K., Tignor, M., Allen, S.K., Boschung, J., Nauels, A., Xia, Y., Bex, V., Midgley, P.M. (Eds.), Climate Change 2013: The Physical Science Basis. Contribution of Working Group I to the Fifth Assessment Report of the Intergovernmental Panel on Climate Change. Cambridge University Press, Cambridge, United Kingdom and New York, NY, USA.
Hatala, J.A. et al., 2012. Greenhouse gas (CO_2, CH_4, H_2O) fluxes from drained and flooded agricultural peatlands in the Sacramento-San Joaquin Delta. Agric. Ecosyst. Environ. 150, 1–18. http://dx.doi.org/10.1016/j.agee.2012.01.009.
Hendriks, D., Dolman, A.J., Van der Molen, M.K., Huissteden, J.V., 2008. A compact and stable eddy covariance set-up for methane measurements using off-axis integrated cavity output spectroscopy. Atmos. Chem. Phys. 8 (2), 431–443.
Herbst, M., Friborg, T., Ringgaard, R., Soegaard, H., 2011. Interpreting the variations in atmospheric methane fluxes observed above a restored wetland. Agric. For. Meteorol. 151 (7), 841–853.
Honaker, J., King, G., Blackwell, M., 2011. Amelia II: a program for missing data. J. Statistical Software 45 (7), 1–47.
Hopfensperger, K.N., Gault, C.M., Groffman, P.M., 2009. Influence of plant communities and soil properties on trace gas fluxes in riparian northern hardwood forests. For. Ecol. Manage. 258 (9), 2076–2082.
Howard, E.A., Gower, S.T., Foley, J.A., Kucharik, C.J., 2004. Effects of logging on carbon dynamics of a jack pine forest in Saskatchewan, Canada. Global Change Biol. 10 (8), 1267–1284.
Hui, D. et al., 2004. Gap-filling missing data in eddy covariance measurements using multiple imputation (MI) for annual estimations. Agric. For. Meteorol. 121 (1), 93–111.
Humphreys, E.R., Andrew Black, T., Morgenstern, K., Li, Z., Nesic, Z., 2005. Net ecosystem production of a Douglas-fir stand for 3 years following clearcut harvesting. Global Change Biol. 11 (3), 450–464.
Huttunen, J.T. et al., 2003. Fluxes of methane, carbon dioxide and nitrous oxide in boreal lakes and potential anthropogenic effects on the aquatic greenhouse gas emissions. Chemosphere 52 (3), 609–621.
Ibrom, A., Dellwik, E., Larsen, S.E., Pilegaard, K., 2007. On the use of the Webb–Pearman–Leuning theory for closed-path eddy correlation measurements. Tellus B 59 (5), 937–946.
Johnson, R.R., McCormick, J.F., 1979. Strategies for Protection and Management of Floodplain Wetlands and Outher Riparian Ecosystems. USDA Forest Service General Technical Report WO$\sim$12.
Kataja-aho, S., Smolander, A., Fritze, H., Norrgård, S., Haimi, J., 2012. Responses of soil carbon and nitrogen transformations to stump removal. Silva Fennica 46 (2), 169–179.
Kauter, D., Lewandowski, I., Claupein, W., 2003. Quantity and quality of harvestable biomass from *Populus* short rotation coppice for solid fuel use—a review of the physiological basis and management influences. Biomass Bioenergy 24 (6), 411–427.
Keenan, R.J., Kimmins, J.P., 1993. The ecological effects of clear-cutting. Environ. Rev. 1 (2), 121–144.
Kolari, P. et al., 2004. Carbon balance of different aged Scots pine forests in Southern Finland. Global Change Biol. 10 (7), 1106–1119.
Kowalski, S., Sartore, M., Burlett, R., Berbigier, P., Loustau, D., 2003. The annual carbon budget of a French pine forest (Pinus pinaster) following harvest. Global Change Biol. 9 (7), 1051–1065.
Kowalski, A.S. et al., 2004. Paired comparisons of carbon exchange between undisturbed and regenerating stands in four managed forests in Europe. Global Change Biol. 10 (10), 1707–1723.
Krause, S., Bronstert, A., Zehe, E., 2007. Groundwater–surface water interactions in a North German lowland floodplain—implications for the river discharge dynamics and riparian water balance. J. Hydrol. 347 (3), 404–417.
Kurz, W.A., Apps, M.J., 1994. The carbon budget of Canadian forests: a sensitivity analysis of changes in disturbance regimes, growth rates, and decomposition rates. Environ. Pollut. 83 (1), 55–61.
Lavoie, M., Kellman, L., Risk, D., 2013. The effects of clear-cutting on soil CO_2, CH_4, and N_2O flux, storage and concentration in two Atlantic temperate forests in Nova Scotia, Canada. For. Ecol. Manage. 304, 355–369.
Law, B.E., Thornton, P.E., Irvine, J., Anthoni, P.M., Van Tuyl, S., 2001. Carbon storage and fluxes in ponderosa pine forests at different developmental stages. Global Change Biol. 7 (7), 755–777.
Lindroth, A., et al., 2012. Clear-cutting is causing large emissions of greenhouse gases-are there other harvest options that can avoid these emissions? EGU General Assembly Conference Abstracts, pp. 7578.
Liu, Y. et al., 2005. Seasonal variation of CO_2 flux and its environmental factors in evergreen coniferous plantation. Sci. China Series D 48, 123–132.
Lloyd, J., Taylor, J.A., 1994. On the temperature dependence of soil respiration. Funct. Ecol. 8, 315–323.
Ma, Y. et al., 2013. Effect of clear-cutting silviculture on soil respiration in a subtropical forest of China. J. Plant Ecol. 6 (5), 335–348.
Machimura, T. et al., 2005. Change of carbon dioxide budget during three years after deforestation in eastern Siberian larch forest. J. Agric. Meteorol. 60 (5), 653–656.
Mäkiranta, P., Laiho, R., Penttilä, T., Minkkinen, K., 2012. The impact of logging residue on soil GHG fluxes in a drained peatland forest. Soil Biol. Biochem. 48, 1–9. http://dx.doi.org/10.1016/j.soilbio.2012.01.005.
Massman, W., 2004. Concerning the measurement of atmospheric trace gas fluxes with open- and closed-path eddy covariance system: the WPL terms and spectral attenuation. In: Lee, X., Massman, W.J., Law, B.E. (Eds.), Handbook of Micrometeorology: A Guide for Surface Flux Measurement. Kluwer Academic Publishers.
Moore, T.R., Knowles, R., 1989. The influence of water table levels on methane and carbon dioxide emissions from peatland soils. Canadian J. Soil Sci. 69 (1), 33–38.
Nave, L.E., Vance, E.D., Swanston, C.W., Curtis, P.S., 2010. Harvest impacts on soil carbon storage in temperate forests. For. Ecol. Manage. 259 (5), 857–866.
Noormets, A. et al., 2012. The role of harvest residue in rotation cycle carbon balance in loblolly pine plantations. Respiration partitioning approach. Global Change Biol. 18 (10), 3186–3201.
Olson, D.M., Griffis, T.J., Noormets, A., Kolka, R., Chen, J., 2013. Interannual, seasonal, and retrospective analysis of the methane and carbon dioxide budgets of a temperate peatland. J. Geophys. Res.: Biogeosci. 118 (1), 226–238.
Paul-Limoges, E., Black, T.A., Christen, A., Nesic, Z., Jassal, R.S., 2015. Effect of clearcut harvesting on the carbon balance of a Douglas-fir forest. Agric. For. Meteorol. 203, 30–42. http://dx.doi.org/10.1016/j.agrformet.2014.12.010.
Rebmann, C. et al., 2012. Data acquisition and flux calculations. In: Aubinet, M., Vesala, T., Papale, D. (Eds.), Eddy Covariance: A Practical Guide to Measurement and Data Analysis. Springer Atmospheric Sciences, pp. 59–84. http://dx.doi.org/10.1007/978-94-007-2351-1_3.
Ren, L. et al., 2002. Methane emission from rice fields in the Chengdu Plain of China. Chinese J. Atmos. Sci. 26 (6), 731–743.
Rosenvald, R., Lohmus, A., 2008. For what, when, and where is green-tree retention better than clear-cutting? a review of the biodiversity aspects. For. Ecol. Manage. 255 (1), 1–15.
Sannigrahi, P., Ragauskas, A.J., Tuskan, G.A., 2010. Poplar as a feedstock for biofuels: a review of compositional characteristics. Biofuels Bioprod. Biorefining 4 (2), 209–226.
Schmid, H.P., 1994. Source areas for scalars and scalar fluxes. Boundary-Layer Meteorol. 67 (3), 293–318.
Schmid, H.P., 2003. Ecosystem–atmosphere exchange of carbon dioxide over a mixed hardwood forest in northern lower Michigan. J. Geophys. Res. 108 (D14). http://dx.doi.org/10.1029/2002JD003011.
Schotanus, P., Nieuwstadt, F., De Bruin, H., 1983. Temperature measurement with a sonic anemometer and its application to heat and moisture fluxes. Boundary-Layer Meteorol. 26 (1), 81–93.
Sevigne, E. et al., 2011. Water and energy consumption of *Populus* spp. bioenergy systems: a case study in Southern Europe. Renew. Sustain. Energy Rev. 15 (2), 1133–1140.
SFA, 2013. General Situation of Forest Resource in China – The 8th National Forest Resources Inventory. China's State Forestry Administration.
Smith, L.K., Lewis Jr, W.M., Chanton, J.P., Cronin, G., Hamilton, S.K., 2000. Methane emissions from the Orinoco River floodplain, Venezuela. Biogeochemistry 51 (2), 113–140.
Subke, J.A., IngliMA, I., Francesca Cotrufo, M., 2006. Trends and methodological impacts in soil CO_2 efflux partitioning: a metaanalytical review. Global Change Biol. 12 (6), 921–943. http://dx.doi.org/10.1111/j.1365-2486.2006.01117.x.
Sun, X., 2000. CH_4 emission flux of forest soils in lower mountain area, Beijing. Soil Environ. Sci. 9 (3), 173–176.
Sun, Q., Zhang, J., Zhou, J., Wu, L., Shan, Q., 2009. Effect of poplar forest on snail control in Dongting Lake area. In: 3rd International Conference on Bioinformatics and Biomedical Engineering, 2009. ICBBE 2009. IEEE, pp. 1–5.
Sun, X., Mu, C., Song, C., Wu, Y., 2011. Effects of cutting on methane flux from forested swamps in Xiaoxing'an Mountains, Northeast China. Chinese J. Soil Sci. 42 (1), 190–194.
Sun, Y., Jiang, H., Zhou, G., Yang, S., Chen, Y., 2013a. Variation characteristics of CO_2 flux in *Phyllostachys edulis* forest ecosystem in subtropical region of China. Chinese J. Appl. Ecol. 24 (10), 2717–2724.
Sun, Q. et al., 2013b. Carbon dioxide and methane fluxes: seasonal dynamics from inland riparian ecosystems, northeast China. Sci. Total Environ. 465, 48–55. http://dx.doi.org/10.1016/j.scitotenv.2013.01.036.
Sun, Z. et al., 2013c. Fluxes of nitrous oxide and methane in different coastal *Suaeda salsa* marshes of the Yellow River estuary, China. Chemosphere 90 (2), 856–865. http://dx.doi.org/10.1016/j.chemosphere.2012.10.004.
Sundqvist, E., Vestin, P., Crill, P., Persson, T., Lindroth, A., 2014. Short-term effects of thinning, clear-cutting and stump harvesting on methane exchange in a boreal forest. Biogeosci. Discussions 11 (3), 4637–4667.
Takagi, K. et al., 2009. Change in CO_2 balance under a series of forestry activities in a cool-temperate mixed forest with dense undergrowth. Global Change Biol. 15 (5), 1275–1288.
Tang, X., Liu, S., Zhou, G., Zhang, D., Zhou, C., 2006. Soil–atmospheric exchange of CO_2, CH_4, and N_2O in three subtropical forest ecosystems in southern China. Global Change Biol. 12 (3), 546–560.
Vann, C.D., Megonigal, J.P., 2003. Elevated CO_2 and water depth regulation of methane emissions: comparison of woody and non-woody wetland plant species. Biogeochemistry 63 (2), 117–134.
Vietto, L., Nervo, G., Facciotto, G., Chiarabaglio, P.M., Coaloa, D., 2011. Activities for sustainable poplar plantations management in Italy. In: Third International Congress on Salicaceae in Argentina.

Wang, D., Chen, Z., Xu, S., 2009. Methane emission from Yangtze estuarine wetland, China. J. Geophys. Res. 114 (G2), G02011.
Webb, E.K., Pearman, G.I., Leuning, R., 1980. Correction of flux measurements for density effects due to heat and water vapour transfer. Quart. J. R. Meteorol. Soc. 106 (447), 85–100.
Williams, C.A., Vanderhoof, M.K., Khomik, M., Ghimire, B., 2014. Post-clearcut dynamics of carbon, water and energy exchanges in a midlatitude temperate, deciduous broadleaf forest environment. Global Change Biol. 20 (3), 992–1007. http://dx.doi.org/10.1111/gcb.12388.
Wright, L., 2006. Worldwide commercial development of bioenergy with a focus on energy crop-based projects. Biomass Bioenergy 30 (8), 706–714.
Wu, Z., Sun, Q., Chen, M., 2001. Biomass and nutrient accumulation of poplar plantation on beach land in Yangtse River in Anhui province. Chinese J. Appl. Ecol. 12 (6), 806–810.
Wu, X. et al., 2011. Long-term effects of clear-cutting and selective cutting on soil methane fluxes in a temperate spruce forest in southern Germany. Environ. Pollut. 159 (10), 2467–2475. http://dx.doi.org/10.1016/j.envpol.2011.06.025.
Xiao, J. et al., 2013. Carbon fluxes, evapotranspiration, and water use efficiency of terrestrial ecosystems in China. Agric. For. Meteorol. 182, 76–90.
Xie, J. et al., 2014. Long-term variability and environmental control of the carbon cycle in an oak-dominated temperate forest. For. Ecol. Manage. 33, 319–328.
Yang, Y. et al., 2005. Effect of clear-cutting on soil respiration of Chinese fir plantation. Acta Pedol. Sin. 42 (4), 584–590.
Zha, T. et al., 2009. Carbon sequestration in boreal jack pine stands following harvesting. Global Change Biol. 15 (6), 1475–1487.
Zhang, R., 2013. Responses of Soil Respiration to Simulated Nitrogen Deposition and Inundation in a *Poplus* Plantation in a Reparian Zone. Chinese Academy of Forestry.
Zhang, X., Qi, L., Zhou, J., Liu, G., Huang, L., 2006. Functions and prospects of forestry ecological engineering on preventing schistosomiasis. World For. Res. 19 (4), 33–37.
Zhao, Z. et al., 2011. Characteristics of CO_2 flux in a Chinese fir plantation ecosystem in Huitong County, Hunan Province. Sci. Silvae Sin. 47 (11), 6–12.
Zona, D. et al., 2009. Methane fluxes during the initiation of a large-scale water table manipulation experiment in the Alaskan Arctic tundra. Global Biogeochem. Cycles 23 (2). http://dx.doi.org/10.1029/2009GB003487.
Zona, D. et al., 2013. Fluxes of the greenhouse gases (CO_2, CH_4 and N_2O) above a short-rotation poplar plantation after conversion from agricultural land. Agric. For. Meteorol. 169, 100–110.